

# FRACTURE AND FAULT DEVELOPMENT IN WERFENIAN QUARTZITIC SANDSTONES – A CASE STUDY FROM THE AUTOCHTHONOUS COVER OF THE TATRA MTS. (POLAND)

Jacek RUBINKIEWICZ & Mirosław LUDWINIAK

*University of Warsaw, Institute of Geology, Laboratory of Tectonics and Geological Mapping, Al. Żwirki i Wigury 93, 02-089 Warsaw, Poland; e-mail: Jacek.Rubinkiewicz@uw.edu.pl, Mirosław.Ludwiniak@uw.edu.pl*

Rubinkiewicz, J. & Ludwiniak, M., 2005. Fracture and fault development in Werfenian quartzitic sandstones – A case study from the autochthonous cover of the Tatra Mts. (Poland). *Annales Societatis Geologorum Poloniae*, 75: 171–187.

**Abstract:** The paper is focused on the analysis of fractures and faults in slightly deformed Werfenian quartzitic sandstones, which in the Polish part of the Tatra Mts. begin the sedimentary succession of the autochthonous cover overlying directly the crystalline core. Investigations including geometric and genetic analysis of fractures and faults have enabled to reconstruct the evolution of the palaeostress field in relation to the generally accepted stages of structural evolution of the Tatra Mts.

The oldest fractures are represented by the S system of shear fractures, which originated due to SSW–NNE compression in almost horizontal or slightly N-tilted beds. The F<sub>1</sub> fault set could have also originated in this stage as a result of slip along the bedding planes or along planes sub-parallel to bedding. This stage took place after the Early Turonian and before the Coniacian. The formation of main zones of strike-slip faults, including the Ornak dislocation zone, could have taken place in the terminal part of this stage or directly after it.

The following stage was linked with rotational uplift of the Tatra Mts., taking place since the Late Miocene. As a result of SSW–NNE extension, the L set of fractures appeared in the gradually uplifted Werfenian rocks. Additionally, the F<sub>2</sub> set of normal faults originated along with the simultaneous opening of some S fractures and reactivation of the F<sub>1</sub> fault set. The last stage of evolution (Pleistocene? – present day) included the formation of landslides, causing rotation of bed complexes together with the fractures. Some F<sub>1</sub> faults could have been reactivated at that time.

**Key words:** fractures, faults, structural analysis, Werfenian, quartzitic sandstones, autochthonous unit, Tatra Mts., Inner Carpathians, Poland.

*Manuscript received 28 December 2004, accepted 4 July 2005*

## INTRODUCTION

This paper is focused on detail analysis of the geometry and origin of systematic fractures (Hancock, 1985) and small-scale faults occurring in Werfenian quartzitic sandstones in the Tatra Mts. The Tatra Mts. are a part of the Inner Western Carpathians which are situated southwards of the Pieniny Klippen Belt (Fig. 1A, B). They are composed of a crystalline core and its sedimentary cover (High-Tatric unit), as well as of higher units overthrust from the south: Križna, Choč and Stražov.

In Poland, the autochthonous cover comprises the Lower Triassic up to the lowermost Upper Cretaceous strata (Fig. 1C). The oldest rocks of the autochthonous cover include Werfenian quartzitic sandstones, lying directly on the crystalline core. In the Western Tatra Mts., the quartzitic sandstones are exposed within a 200 to ca. 900 m wide, E–W trending belt (Guzik, 1959; Bac-Moszaszwili *et al.*, 1979). The sandstones lie directly on the crystalline rocks

covering them from the north; sometimes they also fill in grabens (Jaroszewski 1963, 1965). The study area is located southwards of the Iwaniacka Pass, on the northern consequent slope of the Suchy Wierch Ornaczański Mt. (Fig. 2). Generally, the sandstones are exposed here in gullies and on ridges representing erosional remnants and cuestas, as well as in numerous outcrops above the upper timber line.

This area has been selected for reconnaissance analysis of fractures due to the presence of numerous good outcrops, ubiquitous occurrence of fractures, and particularly because of small tectonic deformations, observed both in the field and on available published maps (Bac-Moszaszwili *et al.*, 1979; Guzik, 1959; Jaroszewski, 1963, 1965; Kotański, 1961; Rabowski, 1959).

The Werfenian strata have been dealt with in numerous papers, with regard to their stratigraphy, sedimentology (Turnau-Morawska, 1955; Roniewicz, 1959, 1963, 1966;

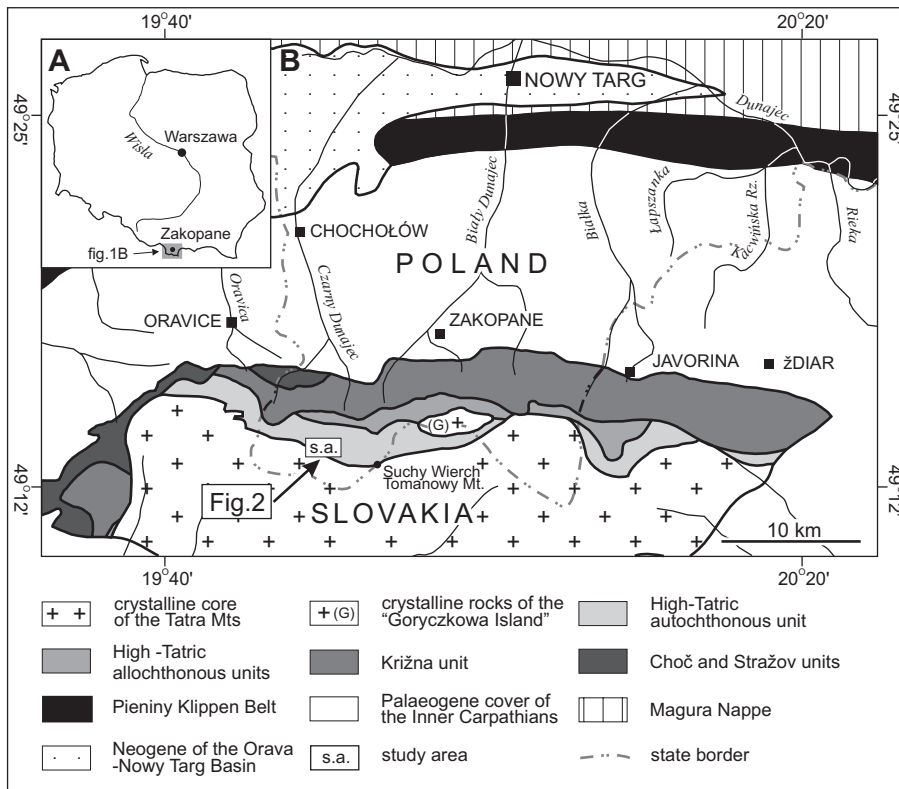
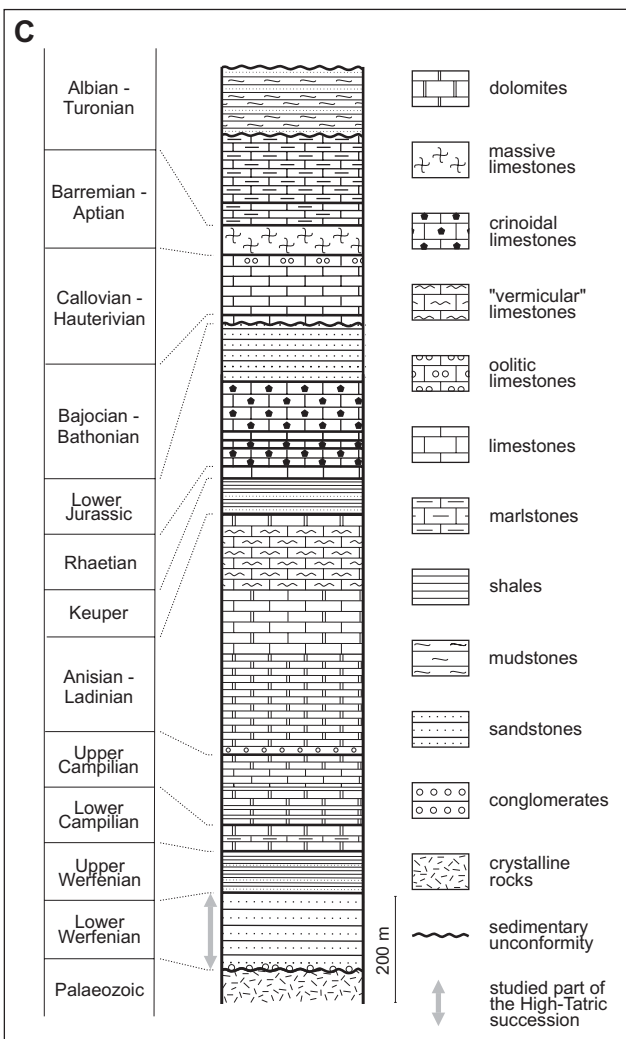


**Fig. 1. A, B** – simplified geological map of the Inner Western Carpathians with location of the study area; **C** – generalised lithostratigraphic log of the High-Tatric succession (compiled and slightly modified from Kotański 1959a, 1961; Lefeld *et al.*, 1985; Uchman, 2004)



Fuglewicz, 1979), and tectonics (Kotański, 1959b, 1961; Rabowski, 1959; Jaroszewski, 1963, 1965, 1967; Piotrowski, 1978). Thus, their occurrence, sedimentary environment and relation to the crystalline core have been recognised; the fractures, however, have not been analysed in detail yet.

Numerous studies of fractures have been conducted in Poland. Of particular importance are papers concerning joints in the Podhale flysch basin (Boretti-Onyszkiewicz, 1968) and the Outer Carpathians (e.g., Książkiewicz, 1968; Aleksandrowski, 1989). The geometry and origin of joints along with palaeostress field reconstruction have recently been presented in a number of papers (e.g., Zuchiewicz & Henkiel, 1993; Zuchiewicz, 1997a, b, 1998; Mastella *et al.*, 1997; Rubinkiewicz, 1998; Mastella & Zuchiewicz, 2000; Mastella & Konon, 2002).

### LITHOLOGY AND STRATIGRAPHY OF THE WERFENIAN SEDIMENTARY SUCCESSION

In the study area, like in other parts of the autochthonous unit, the Werfenian strata lie on peneplained crystalline rocks (Roniewicz, 1963, 1966) (Fig. 1C). The contact is sedimentary in character, with uneven bottom of the Lower Werfenian strata, enveloping the weathered basement surface.

According to Roniewicz (1959, 1966), the Werfenian succession in most cases begins with conglomerates, which are overlain by light quartzitic sandstones intercalated with arkosic sandstones. The bed thickness varies between more

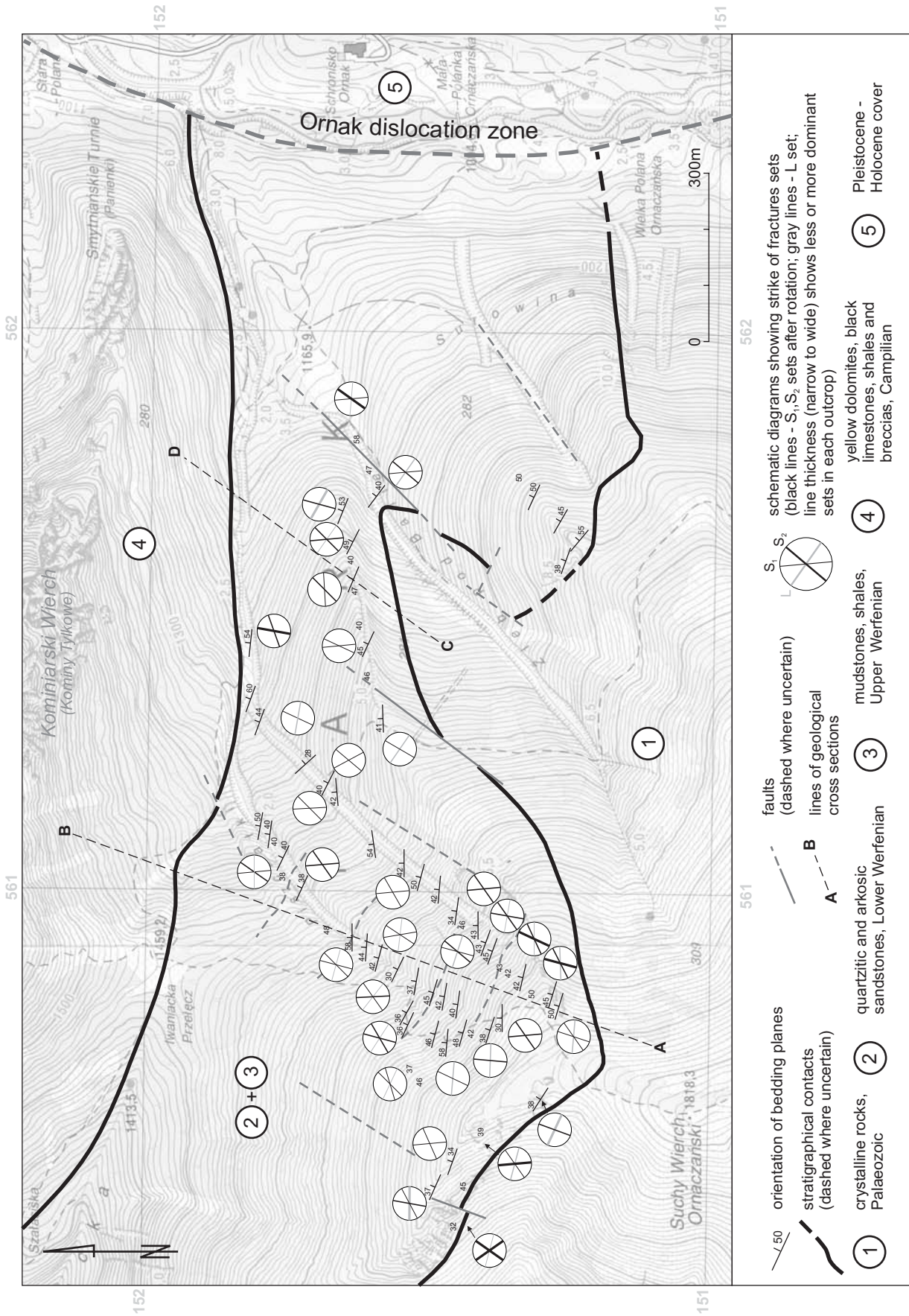


Fig. 2. Structural map of the study area with diagrams showing fracture distribution (some stratigraphical contacts and faults after Jaroszewski, 1965)

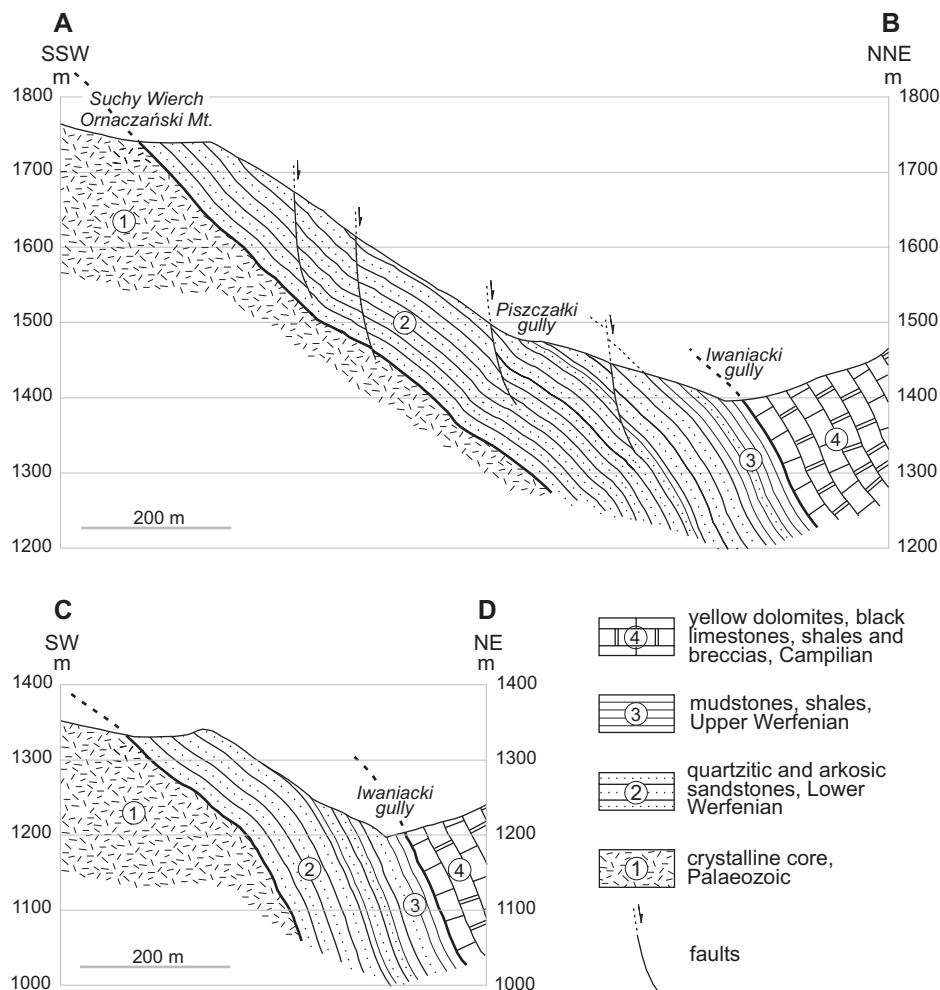


Fig. 3. Geological cross-sections through the study area (for location – see Fig.2)

than ten centimetres to several metres. In the upper part of the succession, brown-coloured, often cross-stratified, quartzitic sandstones intercalate with thin beds of red, rarely green, clayey shales and siltstones. The uppermost member is represented by sandstones with clayey-ferruginous cement, siltstones and clayey shales. The Werfenian deposits are capped by siltstones and clayey shales with intercalations of yellow dolomites, dated to the Campilian (Kotański, 1956, 1959a).

The studied sediments were deposited in a shallow marine basin within a wide littoral zone (Roniewicz, 1959). The material was generally transported from the north (Dżułyński & Gradziński, 1960) and included redeposited clastic material shed from eroded post-Variscan molasses (Lefeld, 1979). The Lower Werfenian deposits lack palaeontological age determinations. Their upper part, in turn, was assigned to the middle part of the Early Triassic basing on megaspore determinations (Fuglewicz, 1979).

According to Roniewicz (1966), the maximal thickness of the Werfenian in the autochthonous units reaches up to 165 m in the vicinity of Osobitá in Slovakia. Following the cross-sections prepared in this study, the maximal thickness of this unit reaches ca. 250 m (Fig. 3 – cross-section A–B) in the study area. However, the genuine thickness may be

slightly smaller due to the presence of numerous faults and landslides.

## METHODOLOGY

During data collection and analysis, selected methodological approaches derived from the studies of joints have been applied (Jaroszewski, 1972; Mastella *et al.*, 1997; Rubinkiewicz, 1998; Mastella & Zuchiewicz, 2000; Mastella & Konon, 2002). The term “joint” is not used here, however, because the majority of fractures are not perpendicular to bedding, as is the case with geometry of most of the joints.

The investigations were carried out in two stages. The first stage included field description of 74 outcrops. Their precise location was determined by a GPS receiver, enabling location with the accuracy of 10–20 m on 1:10,000 topographic maps. The bedding and fracture orientations, as well as bed thicknesses were measured at each outcrop. Following the suggestions of Hancock (1985), Price and Cosgrove (1990), Twiss and Moores (1992), and Dunne and Hancock (1994), cross-cutting relationships, fracture spacing and separation, as well as fissure filling were also

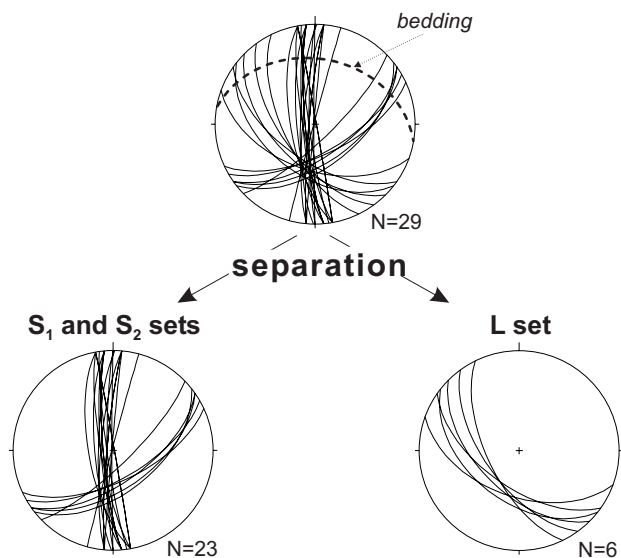


**Fig. 4.** Methodology of separation of fracture sets (example from outcrop no. 2; for location – see Table 1, 2)

studied, alongside with the morphology of fractures, structures occurring on their planes as well as traces of fractures cutting the bedding planes. Infrequent small-scale faults and slickensides were measured and analysed.

The second stage focused on statistical analysis of measurements for every outcrop in the form of plane, point, contour and rose diagrams. In the next step, the data were separated into homogenous subsets (Fig. 4) using TectonicsFP software (Reiter & Acs, 2000; Ortnier *et al.*, 2002). As a result, the fracture sets and systems, extensional and/or shear origin, and relative age were determined for each outcrop. In the final stage, the results from all outcrops were compared, allowing for interpretation of the geometry of particular sets and systems. The palaeostress field was also reconstructed, and followed by a reconstruction of successive stages of fracture formation in the area.

### BEDDING ORIENTATION

Due to relatively low number of bedding orientation data on the existing maps (Guzik, 1959; Bac-Moszaszwili *et al.*, 1979), it is difficult to statistically express their variability in Werfenian rocks of the Western Tatra Mts. The bedding orientation dataset from the autochthonous unit in the Polish part of the Tatra Mts. has already been presented by Jurewicz (2000), basing on both personal and archival data (Jaroszewski, 1963; Piotrowski, 1978). According to that paper, beds orientated 20/42 dominate in the autochthonous unit. Based on the analysis of the intersection line of the Werfenian/Campilian boundary (Bac-Moszaszwili *et al.*, 1979), the generalised strike of these beds has been determined at N100–110°E. Southwards of the Smreczyński Lake and on the northern slopes of Suchy Wierch Tomanowy Mt. (Fig. 1B), the strikes trend E–W (Guzik, 1959). Much more detailed maps by Jaroszewski (1963, 1965) show that in the upper part of the Kościeliska Valley, where E–W trending strikes and dips about 40–55° dominate, the bedding orientations are more variable. According to this author (Jaroszewski, 1963, 1965), the Lower Triassic strata are cut from the east by the Ornak dislocation zone (Fig. 2), also referred to as the Ornak monocline, along which the dips are much more steeper, strikes are almost meridional, and the beds dip suddenly eastwards (Kotański, 1961).

117 bedding orientations were measured in the study area (Fig. 5). These beds are characterised by orientation within 5–30/35–50, dominating at 20/45. The scatter is mainly caused by the presence of faults. The strike-slip faults cause local reorientation of strikes in sub-parallel directions or to azimuths of N125–140°E due to the presence of drag folds. On the northern and north-eastern slope of Suchy Wierch Ornaczański Mt. (Fig. 2), the presence of several consequent structural landslides, resulting from exceeded interbed friction and slip along bedding planes (particularly in those parts of the succession which bear shale intercalations), has been observed. Displacement and rotation of bed complexes takes place within the landslides, what influences the orientation of the measured fractures.

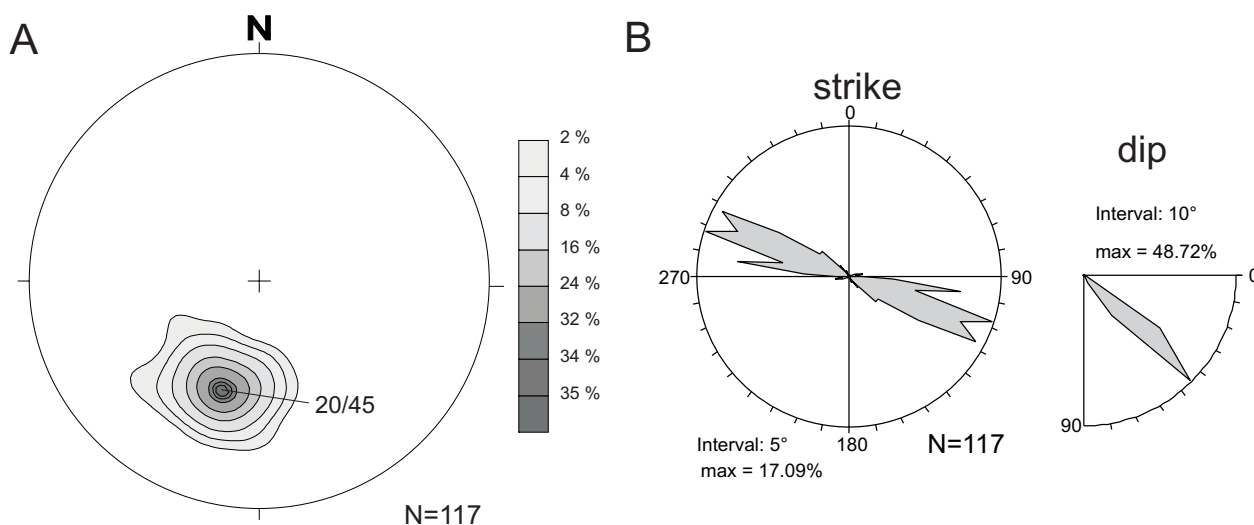


**Fig. 5.** Diagrams of bedding planes. **A** – contour diagram (lower hemisphere); **B** – rose diagrams of strike and dip fluctuations

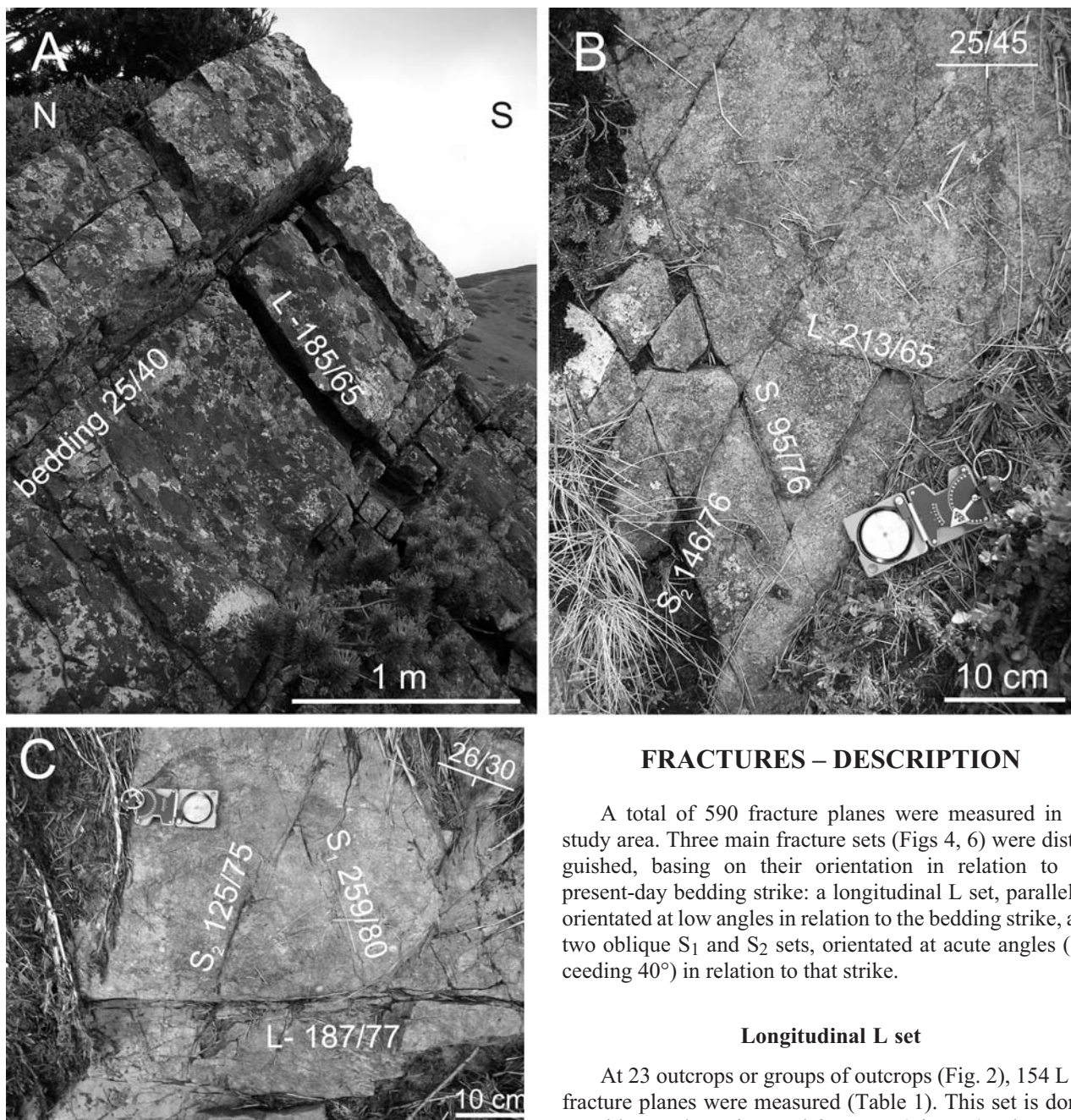


**Fig. 6.** Photographs of selected outcrops bearing fracture sets (for location – see Tables 1, 2). **A** – thick-bedded sandstones with L fracture set – outcrop no. 35; **B** – system of S fractures – outcrop no. 41; **C** – example of cross-cutting relationships between S and L fracture sets – outcrop no. 16

In the study area, consequently with the regional trend (Guzik, 1959), the angle of dip increases slightly northwards (Fig. 3). The northwards increase of dips from  $50^\circ$  to  $80^\circ$  was noted by Rabowski (1959) and Piotrowski (1978) on the southern slopes of the Kominiarski Wierch Mt.

Summing up, the rather uniform bedding orientation (Fig. 5A) allows for a reliable analysis and interpretation of fractures from different outcrops in the study area.

## FRACTURES – DESCRIPTION

A total of 590 fracture planes were measured in the study area. Three main fracture sets (Figs 4, 6) were distinguished, basing on their orientation in relation to the present-day bedding strike: a longitudinal L set, parallel or orientated at low angles in relation to the bedding strike, and two oblique  $S_1$  and  $S_2$  sets, orientated at acute angles (exceeding  $40^\circ$ ) in relation to that strike.

### Longitudinal L set

At 23 outcrops or groups of outcrops (Fig. 2), 154 L set fracture planes were measured (Table 1). This set is dominated by 186/60 orientated fractures (Fig. 7A). The scatter of orientations is  $180\text{--}215/40\text{--}89$ . At solitary outcrops, the L set fracture planes are parallel or sub-parallel ( $\pm 10^\circ$ ) to each other (Fig. 6A, B).

Although at single outcrops the strike orientation of the L set is constant, it displays some variability throughout the study area (Fig. 7A, B). Greater variability can be observed in the case of fracture dips. A part of the analysed fractures are perpendicular to bedding, most of them, however, are not (Fig. 7C).

Surfaces of these fractures are uneven, and traces at which they cut the bedding planes are non-linear, irregular and curved, and change from one to several, rarely some dozen metres. These fractures cut not only single beds, but also groups of beds (Fig. 6A). The mean spacing of the L set fractures varies from more than ten centimetres to 0.5 m. In some cases, the spacing is close (Fig. 6C), between 0.5 cm and several centimetres. The mean separation of fracture

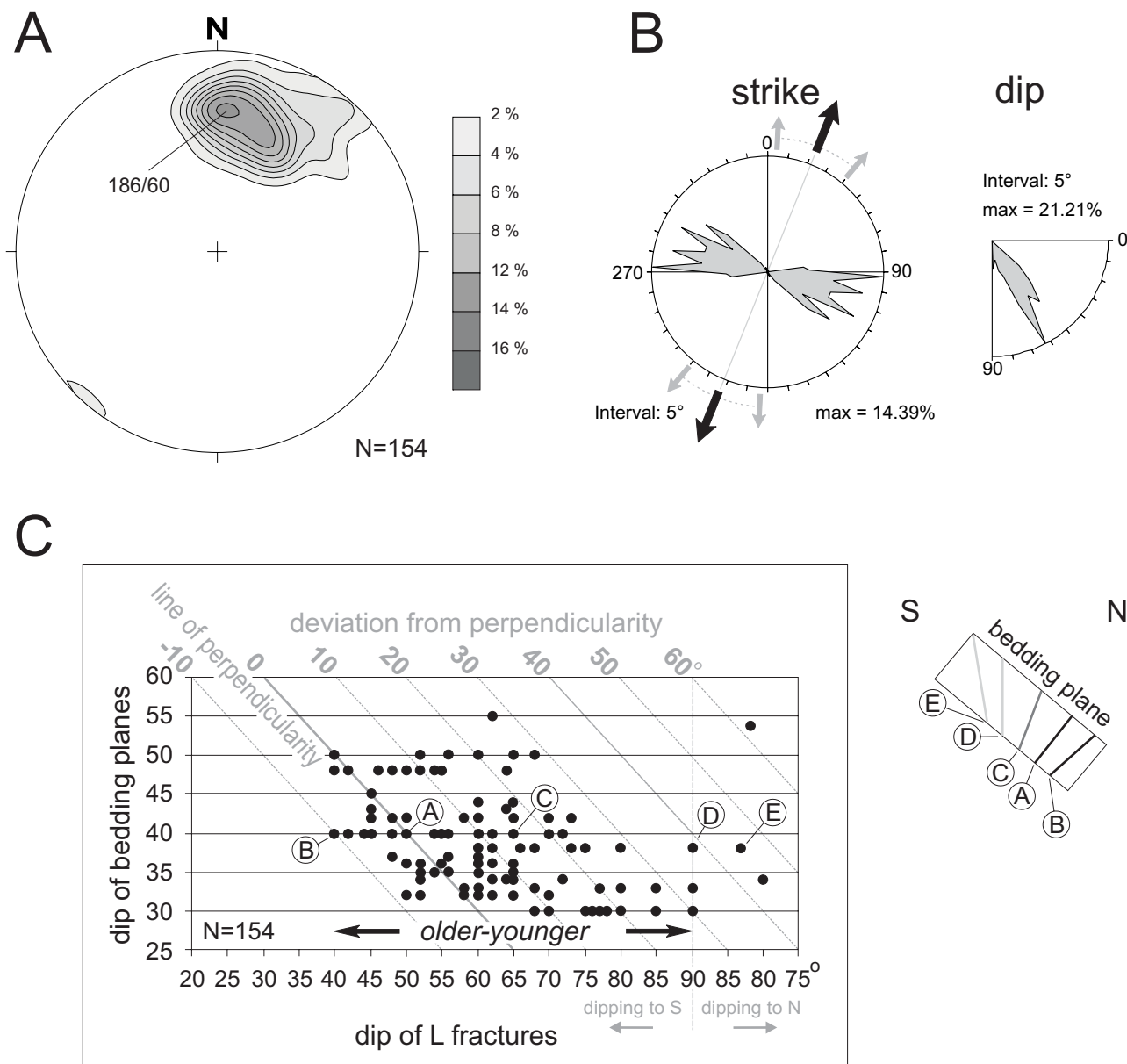


**Fig. 7.** Diagrams showing distribution of L fractures. A – contour diagram (lower hemisphere); B – rose diagrams; C – relationships between the dip of bedding planes and that of L-fractures and deviation from perpendicularity

fissures is between several and more than ten millimetres. Larger separations, exceeding 10 cm, can be observed in thick-bedded sandstones (Fig. 6A). The fractures are typically non-mineralised; only rare crystalline quartz fillings are noted.

The L set fractures occur mainly in the lower part of the succession (Fig. 2). At single outcrops, the L set always co-occurs with other fracture sets. The L fractures generally cut those of S<sub>1</sub> and S<sub>2</sub> sets (Fig. 6C), except for some cases (Fig. 6B).

**Oblique S<sub>1</sub> and S<sub>2</sub> sets**

346 fracture planes of the S<sub>1</sub> and S<sub>2</sub> sets were measured at 26 outcrops (Table 2). The orientation of oblique sets changes throughout different outcrops (Fig. 2). The S<sub>1</sub> set is composed of fractures orientated at 260–310/65–85,

whereas the S<sub>2</sub> set comprises fractures orientated at 120–170/60–80. These sets are usually perpendicular or subperpendicular to bedding, with a deviation of up to 20°. In most outcrops, the two sets co-occur (Figs 4, 6B, C, Fig. 8, Table 2) and form two geometrically arranged groups which cut each other at acute angles of 40–65° (Table 2, Fig. 6B, C, Fig. 8).

The fracture planes of both sets are in most cases flat and smooth. Traces at which they cut bedding planes are rectilinear (Fig. 6B, C), from one to several metres, commonly with an *en echelon* arrangement. In some cases, arc-like transition from the S<sub>1</sub> to S<sub>2</sub> fracture can be observed, alongside with mutually alternating termination.

Sigmoidal and *en echelon* fractures are commonly present on bedding planes (Fig. 8). The length of these fractures is from several to more than ten centimetres. Individual *en echelon* fractures are aligned at 25–40° in relation to their

Table 1

Statistical sheet for L-set fractures

outcrop number	coordinates		number of measurements	bedding planes	L-set average strike	L-set average dip	average extension direction
	X	Y					
2	151526	560838	6	10/35	128	62	38
3	151494	560817	11	12/44	110	52	20
6	151541	560784	9	27/35	120	70	30
8	151516	560701	10	20/35	117	55	27
9	151498	560684	11	25/45	95	52	5
12	151421	560781	4	12/42	95	64	5
15	151278	560800	7	15/45	90	64	0
16	151560	560866	4	26/30	100	76	10
17	151590	560879	2	5/50	105	75	15
25	151767	561073	2	5/40	95	65	5
32	151290	560642	11	33/38	117	74	27
33	151406	560561	8	30/40	100	63	10
34	151458	560531	3	20/34	125	60	35
35	151473	560482	7	25/40	91	59	1
38	151438	560425	14	5/30	132	82	42
39	151283	560824	5	17/50	95	62	5
41	151337	560859	3	6/40	87	65	177
43	151368	560878	3	10/45	112	52	22
55	151727	561226	6	44-60/35	100	68	10
61	151617	561713	7	37/40	126	52	36
62	151669	561685	10	15/55	126	60	36
64	151646	561581	3	25/45	88	45	178
69	151584	561305	8	15/48	110	60	20

array. The  $S_1$  set is dominated by those *en echelon* fractures whose orientation points to dextral movement, whereas the set  $S_2$  comprises fractures indicating sinistral displacement. In some cases the neighbouring *en echelon* fractures are connected by a crack, along which slight displacement can be observed (Fig. 8A- $S_2$  array).

The fracture spacing for both sets varies between ten to twenty centimetres and several tens of centimetres. The separation, in turn, reaches an average of several millimetres. These fractures are commonly mineralised by crystal-line quartz.

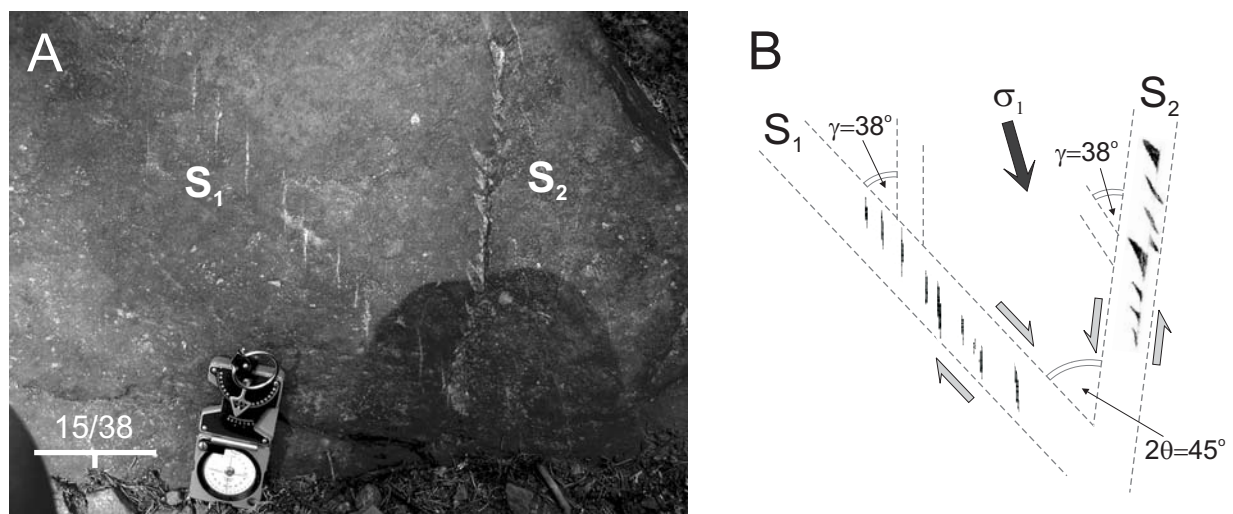


Fig. 8. Detailed view of the S fracture system bearing *en echelon* vein arrays ( $2\theta$  – double shear angle,  $\gamma$  – vein array angle)

Table 2

Statistical sheet for S-system fracture

exposure number	coordinates		number of measurements	bedding planes	azimuth of rotation axis	rotation angle	after rotation		double shear angle	compression direction
	X	Y					S <sub>1</sub> set average strike	S <sub>2</sub> set average strike		
2	151526	560838	23	10/35	96	34	177	65	68	31
3 5	151494	560817	22	12/44	101	43	45	15	30	30
6 7	151541	560784	23	27/35	117	21	12	55	43	33
8	151516	560701	15	20/35	126	40	45	84	39	64
9 11	151498	560684	16	25/45	116	20	163	27	44	5
12	151421	560781	13	12/42	100	34	0	25	25	13
13	151390	560761	9	15/40	93	24	178	58	60	28
15	151278	560800	24	15/45	90	30	15	65	50	40
16	151560	560866	8	26/30	118	19	165	35	50	10
17 20	151590	560879	7	5/50	104	27	40	10	30	25
23	151760	561037	10	25/40	118	25	165	55	70	20
25 26	151767	561073	11	5/40	93	20	175	35	40	15
29	151832	561447	13	6/54	111	43	5	70	65	38
33	151406	560561	26	30/40	114	24	0	60	60	30
34	151458	560531	13	20/34	108	27	170	65	75	27
35	151473	560482	12	25/40	132	35	5	60	55	32
39	151283	560824	7	17/50	110	36	5	65	60	35
41	151337	560859	18	6/40	83	29	34	64	30	49
43 44	151368	560878	13	10/45	100	42	10	58	48	34
45	151405	560918	13	20/40	85	37	176	63	67	30
50 51	151516	561027	7	15/50	75	31	5	63	58	34
53	151668	561179	6	355/42	78	43		47		
54	151687	561195	8	27/40	106	42	170	50	60	20
59	151645	561801	13	50/57	149	26	63	100	37	82
63	151644	561636	10	22/50	116	40	165	45	60	15
64 65	151646	561581	6	25/45	123	49	175	55	60	25

## FRACTURES – INTERPRETATION

### Longitudinal L set

The observed statistically insignificant variability of the orientation of L set fractures does not allow for tracing any regional regularities (Fig. 2). One of the reasons for such variability is the activity of landslides, causing the planar rotation (rotation axis perpendicular to bedding) of beds with the co-occurring fractures. However, bedding planes do not change their strike and dip.

Analysis of the traces at which the fractures cut the bedding planes (Hancock, 1985; Dunne & Hancock, 1994) indicates that the L fractures are younger than those of S<sub>1</sub> and S<sub>2</sub> sets. The relatively younger age of these fractures may be indirectly testified to by the almost complete lack of mineralisation along the longitudinal set, whereas older fractures commonly reveal stronger mineralisation (cf. Price & Cosgrove, 1990). Uneven, irregular fracture planes and the commonly curvilinear shape of their traces on the bedding planes point to their extensional origin.

According to Price (1956, 1966), typical vertical extensional fractures are formed when the axis of the lowest stress  $\sigma_3$  is orientated horizontally and lies perpendicular to

the fracture planes. Thus, the continuous spectrum of variability of the dip of L set (Fig. 7) suggests that most probably the fractures could have been formed gradually during a long interval. Such a mechanism could have taken place during the gradual tilting of bedding. This, in turn, could have led to the formation of fractures A and B (Fig. 9), sub-perpendicular to bedding and presently dipping at 40–60° (Fig. 7C). This event probably occurred when the Lower Werfenian sandstones were in an almost horizontal position (Fig. 9). Slightly younger are fractures C (Fig. 9), deviated from the perpendicularity to bedding by 10–25° (Fig. 7C), situated at higher angles in their present-day position and dipping 60–80°. Finally, the youngest fractures appear to be D and E (Fig. 9), the surfaces of which are at present vertical or subvertical. The gradual northwards tilting of the Werfenian beds during horizontal extension caused the younger fractures to reveal larger deviation from perpendicularity to bedding (Fig. 7C, 9).

The L fractures commonly occur in the lower part of the quartzitic sandstones. This might be a result of the fact that during the rotational uplift of the Tatra Mts. the overburden was removed first from that part of the succession, resulting in stress release in the rock massif and the subsequent formation of L fractures.

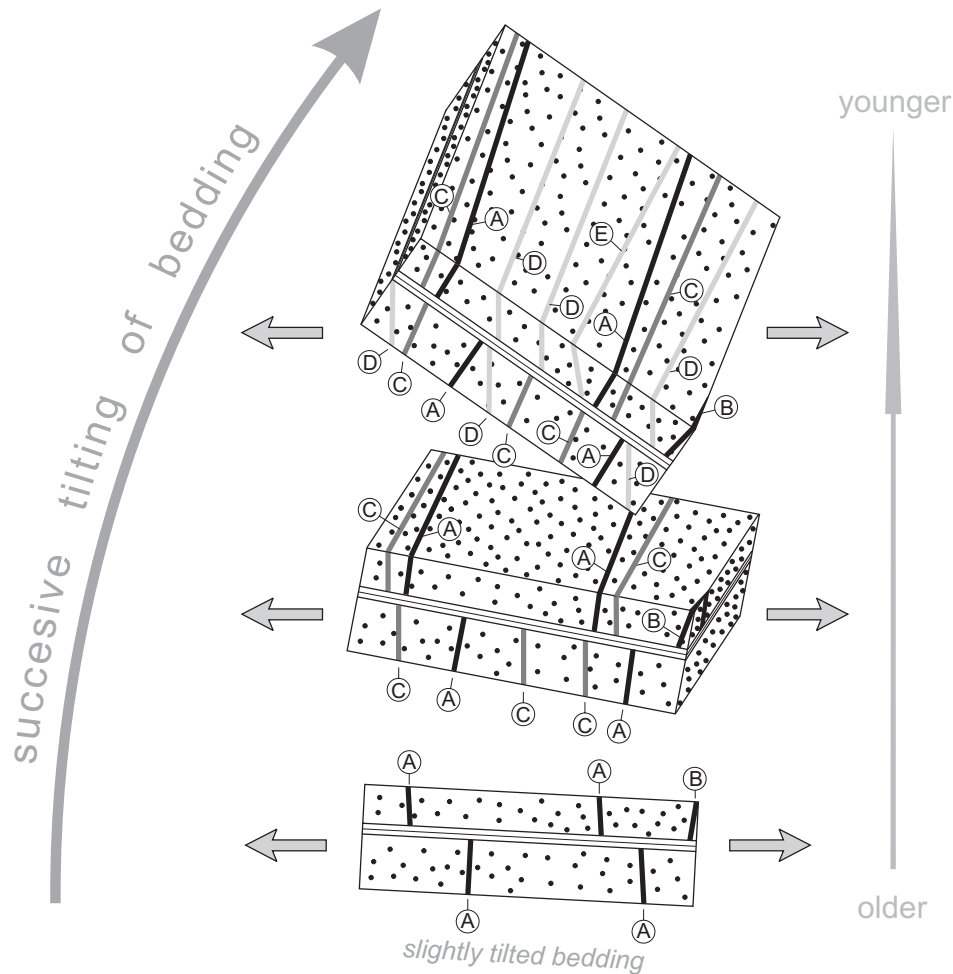


**Fig. 9.** Scheme showing the development of L fractures. Continuous extensional regime with successive tilting of the Tatra massif along the Sub-Tatric fault

The locally observed increase in the density of L fractures is caused by their occurrence in longitudinal zones (WNW–ESE) of normal faults (Figs 2, 3 – A–B cross-section). This close spacing of fractures has also been described by Piotrowski (1978) from the upper part of the autochthonous unit.

#### Oblique $S_1$ and $S_2$ sets

The properties of  $S_1$  and  $S_2$  fractures described above indicate that they are typical shear fractures which were formed due to compression. These sets form a system of conjugate and complementary fractures (Hancock, 1985; Mastella & Zuchiewicz, 2000), along which either arrays of *en echelon* fractures (Fig. 8) or a complete disruption of the rock mass (Fig. 6B, C) took place.

The orientation of the acute dihedral (orientation of the maximum principal stress axis  $\sigma_1$ ) and the values of the acute angle ( $2\theta$ ), i.e. the double shear angle, were analysed (Fig. 10). The initial orientation of the largest principal stress axes for the shear fracture system are typically horizontal (Hancock, 1985; Jaroszewski, 1972); therefore, it was necessary to rotate the fractures to reconstruct their primary position from the stage of their formation, like in case of shear joints (i.e., Mastella *et al.*, 1997).

The question of rotation methodology was discussed in many papers dealing with jointing in the Outer Carpathians (Książkiewicz, 1968; Mastella, 1988; Rubinkiewicz, 1998; Zuchiewicz, 1998; Mastella & Zuchiewicz, 2000; Mastella & Konon, 2002). One of the possible solutions (in the case of fractures perpendicular to bedding) is the application of dip angle rotation along bedding strike (Murray, 1967; Rubinkiewicz, 1998; Zuchiewicz, 1998; Mastella &

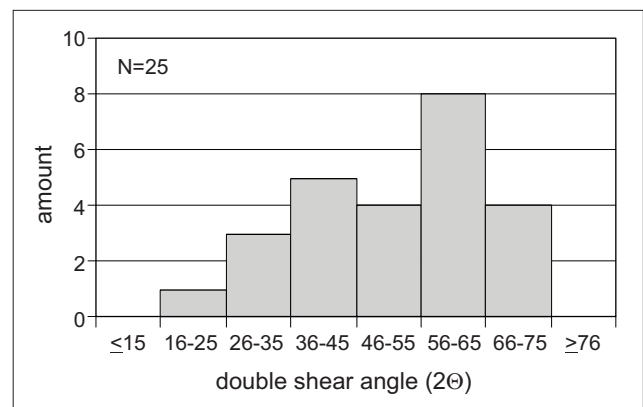


**Fig. 10.** Histogram of the double shear angle variability

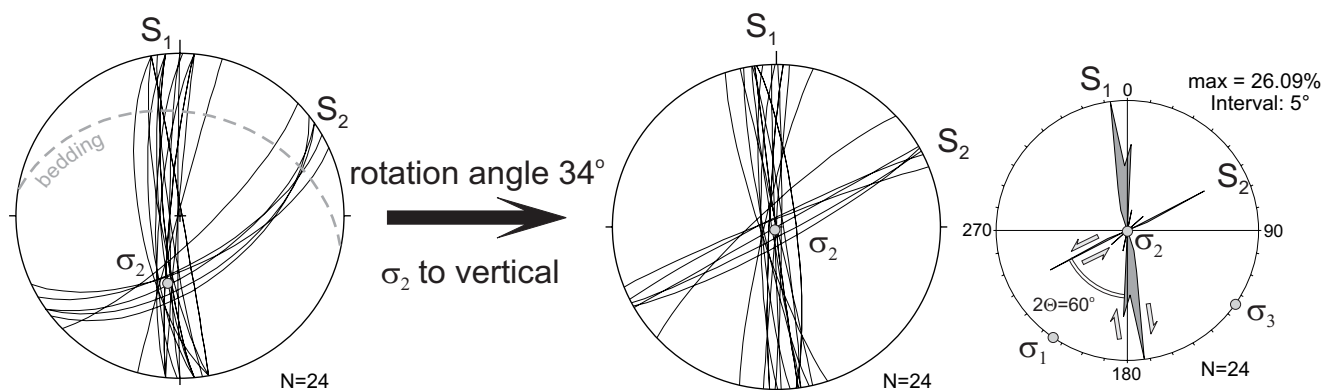


**Fig. 11.** Methodology of rotation of shear fractures  $S_1$  and  $S_2$  (example from outcrop no. 2 – see text for explanation)

Zuchiewicz, 2000; Mastella & Konon, 2002; Śmigielski, 2003). In zones of high tectonic involvement it is indispensable to apply such rotation, which would include plunge correction (Rubinkiewicz, 1998). Another method (in case of the Tatra Mts.) is the application of the rotation proposed by Jurewicz (2000), including the plunge of the Tatra block (rotation axis  $90^\circ$ , angle  $40^\circ$ ). The first method cannot be applied in the study area because of the non-perpendicularity to bedding of some oblique sets in many outcrops. In turn, when the second method is applied, a large dispersion of the obtained orientations is observed, and the main stress axes for this fracture system still display some plunge after rotation. In the study area, both sets ( $S_1$ ,  $S_2$ ) co-occur in most outcrops (Table 2). Therefore, a third method, including rotation of the plunging  $\sigma_2$  stress axis (axis at which both sets intersect one another) to a position at which it attains a vertical position, has been applied (Fig. 11; cf. Price, 1959; Książkiewicz, 1968; Mastella, 1988). After such rotation, the surfaces of the shear system fractures attained a vertical position with a deviation of  $\pm 10^\circ$ ; therefore, their dips need not have to be analysed statistically (Fig. 11). The applied rotation mode indicates that the shear fractures were formed in horizontal or slightly tilted beds, dipping at  $0\text{--}15^\circ$  to the North.

The orientation of  $\sigma_1$  stress axis at individual outcrops displays some variability, although the SSW–NNE compression does prevail (Fig. 12).

In particular outcrops, the double value of shear angle between sets  $S_1$  and  $S_2$  varies between  $25^\circ$  and  $75^\circ$  (Table 2), whereas the dominating values are  $56\text{--}65^\circ$  and  $36\text{--}45^\circ$  (Fig. 10). According to Hancock (1985), values comprised in the first range point to shear fractures. The second range, with lower values of the double shear angle, indicates hybrid-shear origin of fractures. Variability of the double shear angle influences the variable orientation of  $S_1$  and  $S_2$  sets.

In some cases, a change of orientation of the entire system can be observed (Fig. 2) as a result of either dragging in strike-slip fault zones, or of landsliding.

### FAULTS – DESCRIPTION

There are no determined large fault zones on maps covering the study area (Guzik, 1959; Bac-Moszaszwili *et al.*,

1979). Detailed geological studies conducted in adjacent areas (Piotrowski, 1978; Bac-Moszaszwili, 1998), however, point to the importance of fault tectonics.

The transverse Ornak dislocation zone of fault or flexure character bounds the study area from the east (Jaroszewski, 1963, 1965) (Fig. 2). Along this zone, the Lower Triassic strata are in their eastern part shifted southwards (Bac-Moszaszwili *et al.*, 1979), what might indicate that this is a zone of a dextral strike-slip fault or a dip-slip fault with the downthrown eastern side. Southwards of the study area, Siwe Skąły tectonic graben occurs (Jaroszewski, 1963), bounded by steep dip-slip faults. An isolated patch of quartzitic sandstones is preserved in this graben.

Basing on geological maps (Jaroszewski, 1963), an analysis of the Werfenian/crystalline core boundary, interpretation of aerial photographs, and local diversity of bedding strikes (caused by fault dragging), the presence of several main faults has been determined in the study area (Fig. 2). They form a NE–SW orientated fault set, most probably of strike-slip and dip-slip character, cutting both autochthonous rocks and the crystalline core.

A total of 14 fault planes (Figs 13, 14) have been measured in the outcrops. Two sets  $F_1$  and  $F_2$  of longitudinal nor-

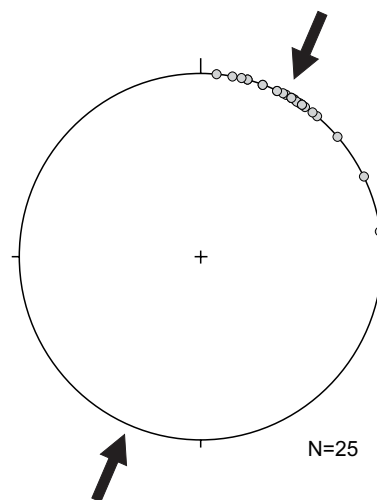


**Fig. 12.** Diagram of compression directions inferred from selected outcrops (cf. also Table 2; black arrows indicate average direction of compression)

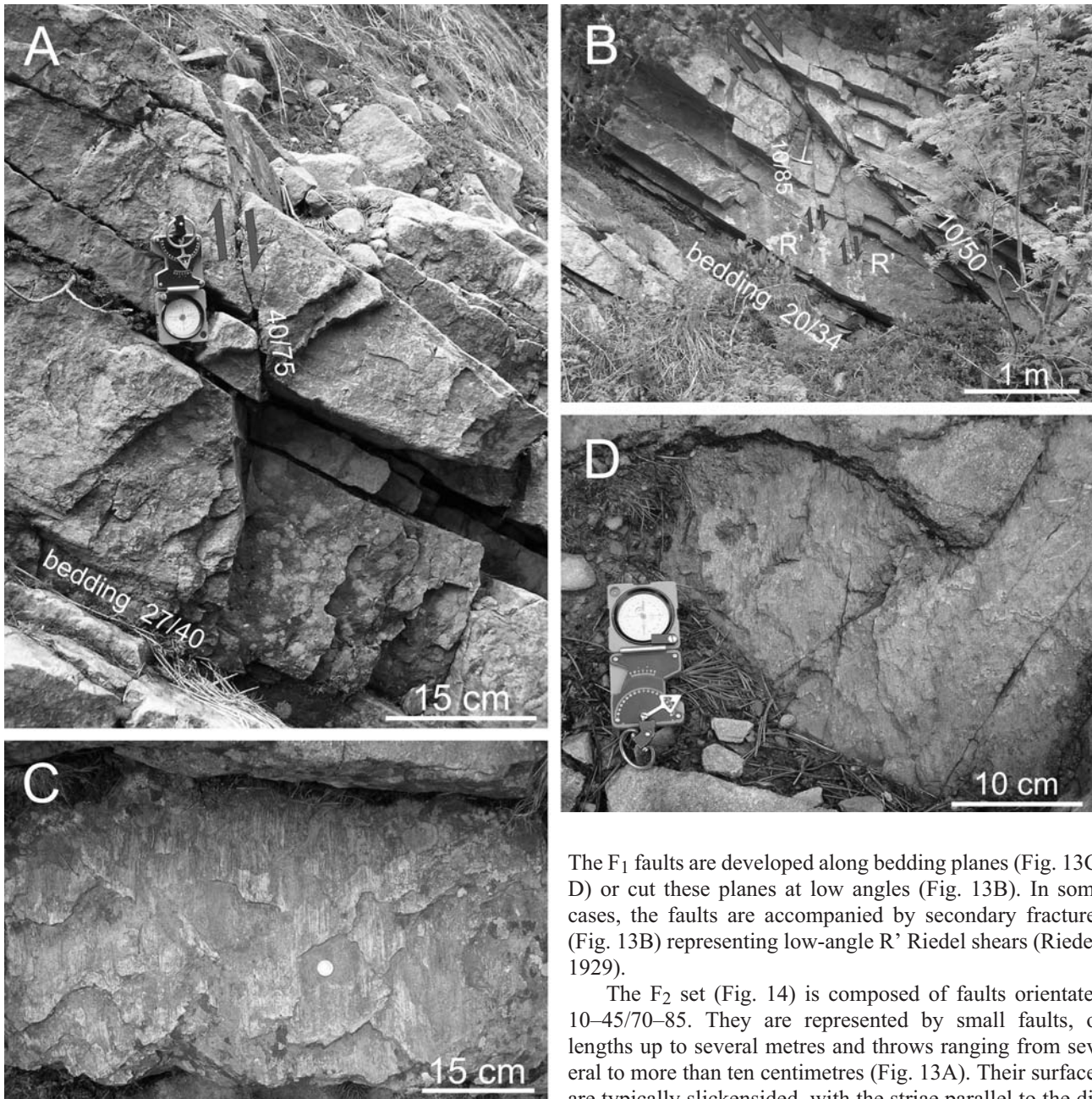


**Fig. 13.** Photographs of selected fault-bearing outcrops. **A** – steeply-dipping normal fault ( $F_2$ -set) – outcrop no. 54; **B** – normal fault with Riedel shears ( $F_1$ -set) – outcrop no. 48; **C** – slickensided surface – example from the tourist route; **D** – slickensided surface cutting S fractures – outcrop no. 6

mal faults orientated parallel or sub-parallel to bedding have been distinguished.

The  $F_1$  set (Fig. 14) comprises faults striking  $350-10/30-50$ . Despite their rare occurrence in the outcrops (5 measurements), their presence throughout the study area is indicated by the large number of slickensided surfaces of quartzitic sandstones observed in the debris and on the tourist route. The fault planes are slickensided (Fig. 13 C, D), with well visible striae and quartz mineralisation. The observed separation is from several to more than ten metres.

The  $F_1$  faults are developed along bedding planes (Fig. 13C, D) or cut these planes at low angles (Fig. 13B). In some cases, the faults are accompanied by secondary fractures (Fig. 13B) representing low-angle  $R'$  Riedel shears (Riedel, 1929).

The  $F_2$  set (Fig. 14) is composed of faults orientated  $10-45/70-85$ . They are represented by small faults, of lengths up to several metres and throws ranging from several to more than ten centimetres (Fig. 13A). Their surfaces are typically slickensided, with the striae parallel to the dip (Fig. 14). In some cases, a denser pattern of L fractures is observed in rocks directly adjacent to these faults.

## FAULTS – INTERPRETATION

The origin of  $F_1$  faults may be linked with two possible stages. In the older stage, associated with Alpine folding, the faults were formed on anisotropy surfaces sub-parallel to the bedding planes as an effect of bed movement against each other. The primary orientation of such faults (before tilting) must have been close to horizontal (Fig. 14). In the younger stage, during the rotational uplift of the Tatra crystalline core, some of the faults were reactivated. They were also reactivated as a result of gravitational slip on consequent slopes of the Suchy Wierch Ornaczański Mt.

The orientation of compression determined for the faults formed during the first stage was SSW–NNE

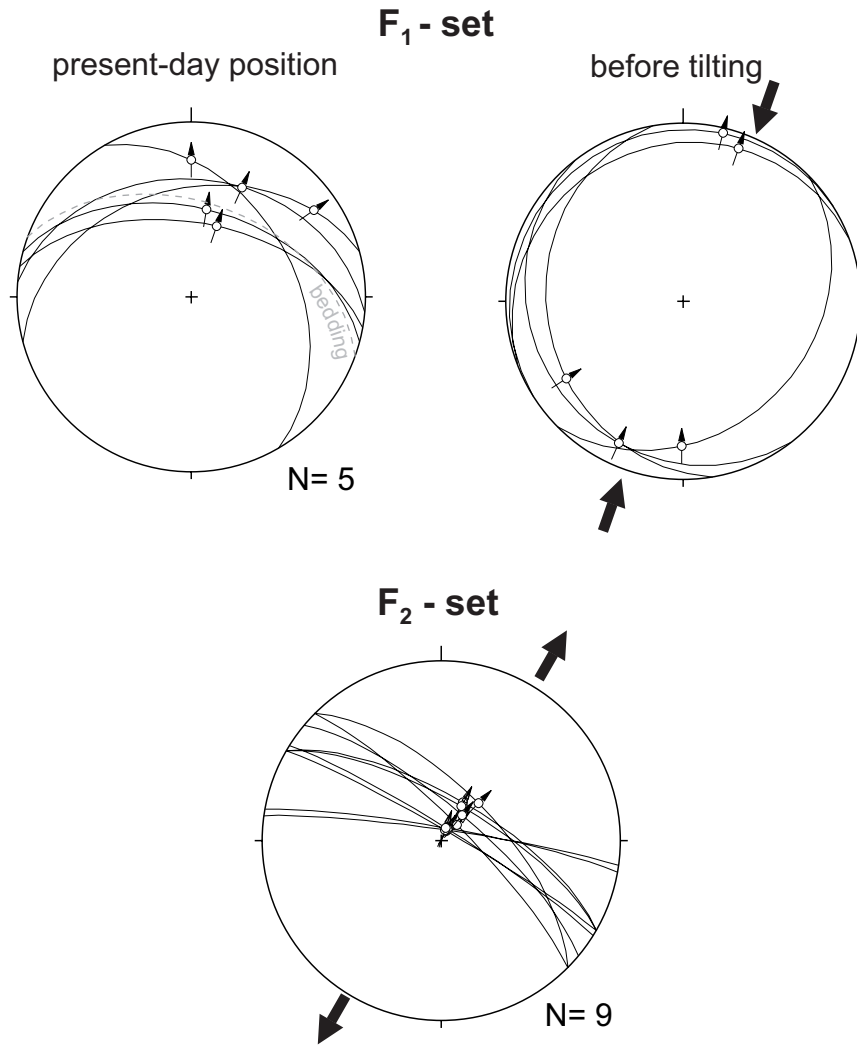


**Fig. 14.** Angelier's diagrams of  $F_1$  and  $F_2$  fault sets (black arrows indicate average direction of compression for  $F_1$  and extension for  $F_2$ )

(Fig. 14). Similar orientations, based on slickensides, have been interpreted for the High-Tatric autochthonous unit by Piotrowski (1978). Infrequent fold axes, measured in the upper part of the Werfenian eastwards of Iwaniacka Pass and southwards of Panienki (Fig. 2), indicate an orientation of N100–110°E (Kotanski, 1961; Piotrowski, 1978). These folds display northern vergence; thus, tectonic transport must have taken place from the SSW to the NNE (within an interval of N10–20°E).

The  $F_2$  faults probably accompany larger zones of steep normal faults (Fig. 3). In the morphology of the northern slopes of Suchy Wierch Ornaczański Mt., step-like breaks of slope, either lithologically-controlled or associated with the  $F_2$  faults, can be observed. A similar fault set occurs farther to the north, e.g. in the Hala na Stołach alp (Bac, 1963). The discussed set was formed during the SW–NE orientated extension (Fig. 14).

## CONCLUSIONS

An analysis of the network of fractures and faults indicates that they are arranged in geometrical sets and systems,

formed in specific stress fields which affected the Werfenian rocks in the study area.

The evolution of the analysed discontinuous structures in relation to the structural development of the Tatra Mts. proceeded through several stages (Fig. 15).

The main episode of folding of the sedimentary cover of the Tatra Mts. took place after the Early Turonian and prior to the Coniacian (Lefeld, 1997), when the High-Tatric and Sub-Tatric rock series became thrust to the north, on the autochthonous unit. Rocks of the latter unit, including the Werfenian, were subject to compression (Fig. 15A). Small tilting or rotation could have taken place during tectonic transport. In this stage, the formation of the S system of shear fractures in horizontal or slightly N-tilted beds took place along with their mineralisation. Fractures of this system originated due to SSW–NNE to SW–NE orientated compression. After that, the movement of beds could have taken place along bedding planes, causing the formation of  $F_1$  fault as a result of SSW–NNE orientated compression (Fig. 15B). In the following stage, at similar direction of compression, strike-slip fault zones, including the Ornak dislocation zone (Fig. 2), were formed. The difference between the generally northwards thrusting and direction of

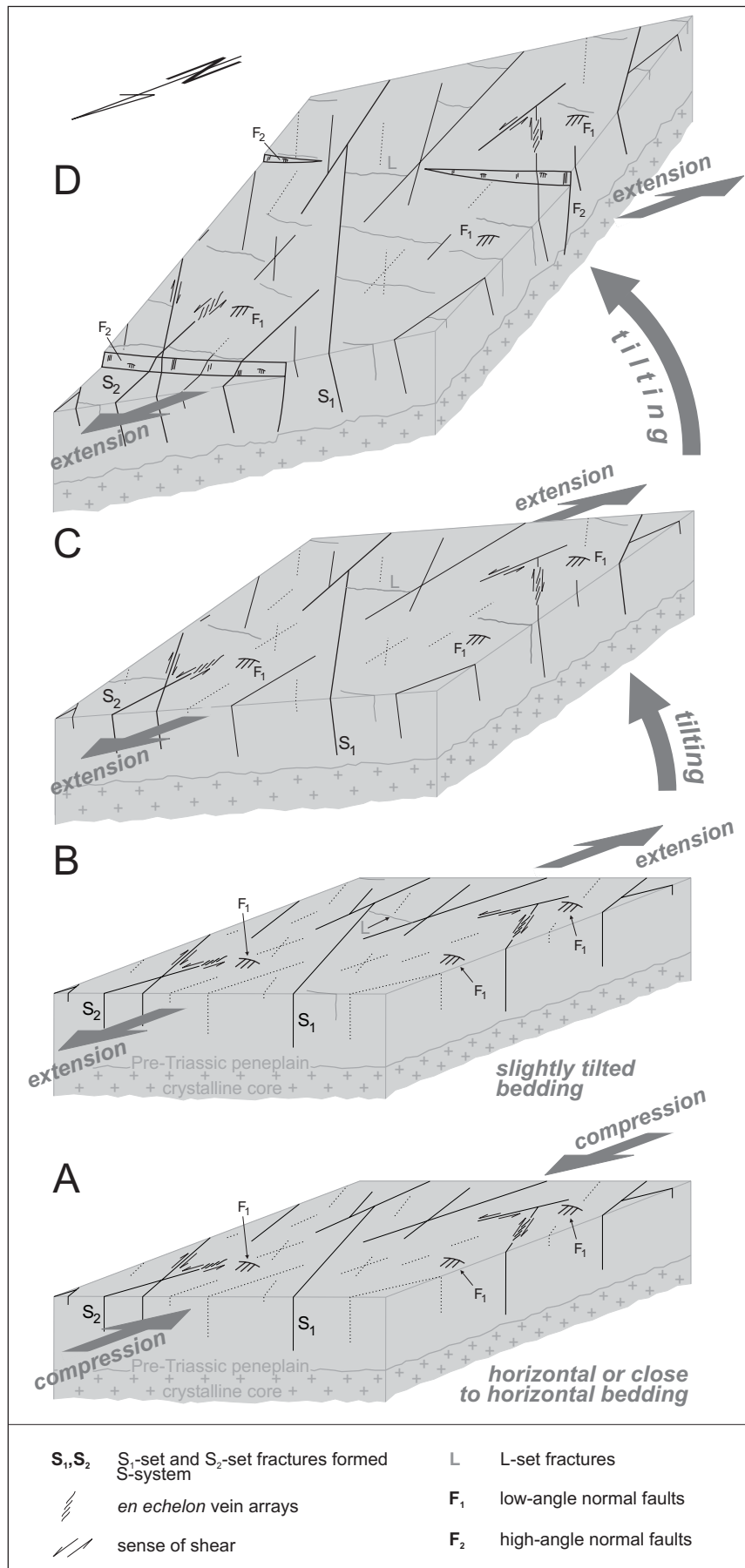


Fig. 15. Scheme of consecutive stages of development of fractures and faults

compression inferred from the S fractures and F<sub>1</sub> faults could be a result of either local change of the thrusting direction or later horizontal rotation of the Tatra Mts. (Grabowski, 1997).

In the Late Miocene, rotational tilting of the Tatra Mts. crystalline core with its sedimentary cover to the north was linked with either uplift (Burchart, 1972; Král, 1977; Vaškovič, 1977; Kováč *et al.*, 1994) or pop-up (Sperner *et al.*, 2002) of the Tatra massif along the southern Sub-Tatric fault (Andrusov, 1959). During this stage (Fig. 15B–D), the non-mineralised extensional set of L fractures (SSW–NNE orientated extension) and steep normal F<sub>2</sub> faults were formed. At the same time, secondary displacement (reactivation) along the planes of F<sub>1</sub> faults and strike-slip faults took place, being accompanied by extensional opening of the S fracture system.

The last stage (Pleistocene?–Present) is linked with the formation of landslides and, most probably, reactivation of some F<sub>1</sub> faults. Within the landslides, rotation of beds or their complexes could have taken place, influencing the geometry of the fracture and fault network.

The presence of the described discontinuous structures, mainly faults, as well as the occurrence of landslides greatly influences determination of the real thickness of the Werfenian quartzitic sandstones. Therefore, the maximal thickness determined at ca. 250 m is much larger than that suggested by other authors (Roniewicz, 1997).

The presented evolution of faults and fractures refers only to the study area. Therefore, it cannot be excluded that the analysed area lies within a block which had undergone rotation (e.g. along large zones of strike-slip faults). Such a rotation could have biased the results of stress field interpretation. The results of this study are, therefore, of preliminary character, and can form a basis for further detailed examination of other exposures of Werfenian rocks, as well as the upper parts of the High-Tatric autochthonous unit and the Sub-Tatric units.

### Acknowledgements

The authors would like to thank Prof. Leonard Mastella, Prof. František Markó and an Anonymous Reviewer for their critical remarks. This study was supported by a grant of the Institute of Geology, University of Warsaw (BST-977/2).

### REFERENCES

- Aleksandrowski, P., 1989. Structural geology of the Magura nappe in the Mt. Babia Góra region, Western Outer Carpathians. (In Polish, English summary). *Studia Geologica Polonica*, 96: 1–140.
- Andrusov, D., 1959. *Geológia Československých Karpat. Zväzok I*. (In Slovak). Bratislava, 375 pp.
- Bac, M., 1963. The geology of the Stoły massif in the West Tatras. (In Polish, English summary). *Acta Geologica Polonica*, 13: 61–89.
- Bac-Moszaszwili, M., 1998. Geology of the Subatric units, Western Tatra Mts., Poland. (In Polish, English summary). *Studia Geologica Polonica*, 111: 113–136.
- Bac-Moszaszwili, M., Burchart, J., Głazek, J., Iwanow, A., Jaroszewski, W., Kotański, Z., Lefeld, J., Mastella, L., Ozimkowski, W., Roniewicz, P., Skupiński, A. & Westwalewicz-Mogilska, E., 1979. *Geological map of the Polish Tatra Mountains 1: 30,000*. Wydawnictwa Geologiczne, Warszawa.
- Birkenmajer, K., 1986. Stages of structural evolution of the Pieniny Klippen Belt, Carpathians. *Studia Geologica Polonica*, 88: 7–32.
- Boretti-Onyszkiewicz, W., 1968. Joints in the flysch of western Podhale. (In Polish, English summary). *Acta Geologica Polonica*, 18: 101–152.
- Burchart, J., 1972. Fission-track age determinations of accessory apatite from the Tatra Mts, Poland. *Earth and Planetary Science Letters*, 15: 418–422.
- Dunne, W. M. & Hancock, P. L., 1994. Paleostress analysis of small-scale brittle structures. In: Hancock, P. L. (Ed.), *Continental Deformation*. Pergamon Press, Cambridge: 101–120.
- Dzulyński, S. & Gradziński, R., 1960. Source of Lower Triassic clastics in the Tatra Mts. *Bulletin de l'Academie Polonaise des Sciences, serie des sciences géologiques et géographiques*, 8: 45–48.
- Fuglewicz, R., 1979. Megaspores found in the earliest Triassic of Poland. *Rocznik Polskiego Towarzystwa Geologicznego*, 49: 271–275.
- Grabowski, J., 1997. Paleomagnetic results from the cover (High Tatric) units and the nummulitic Eocene in the Tatra Mts (Central West Carpathians) and their tectonic implications. *Annales Societatis Geologorum Poloniae*, 67: 13–23.
- Guzik, K., 1959. *Mapa geologiczna Tatr 1: 10 000, arkusz B2: Kominy Tylkowe*. (In Polish). Wydawnictwa Geologiczne, Warszawa.
- Hancock, P. L., 1985. Brittle microtectonics: principles and practice. *Journal of Structural Geology*, 7: 437–457.
- Jaroszewski, W., 1963. Tectonics of the High-Tatric series in the upper floor of the Kościeliska Valley in the Tatra Mountains. (In Polish, English summary). *Acta Geologica Polonica*, 13: 43–58.
- Jaroszewski, W., 1965. Geology of the upper part of Kościeliska Valley in the Tatra Mts. (In Polish, English summary). *Acta Geologica Polonica*, 15: 429–499.
- Jaroszewski, W., 1967. Geological observations on the rocks of the upper part of the Kościeliska Valley in the Tatra Mts. (In Polish, English summary). *Biuletyn Geologiczny Wydziału Geologii Uniwersytetu Warszawskiego*, 9: 217–271.
- Jaroszewski, W., 1972. Mesoscopic structural analysis of the tectonics of non-orogenic areas, with the northeastern Mesozoic margin of the Święty Krzyż Mountains as an example. (In Polish, English summary). *Studia Geologica Polonica*, 38: 1–216.
- Jurewicz, E., 2000. Tentative correlation of the results of structural analysis in the granitoid core and nappe units of the Tatra Mts. (southern Poland). (In Polish, English summary). *Przegląd Geologiczny*, 48: 1014–1018.
- Kováč, M., Kral, J., Márton, E., Plašienka, D. & Uher, P., 1994. Alpine uplift history of the Central Western Carpathians: geochronological, paleomagnetic, sedimentary and structural data. *Geologica Carpathica*, 45: 83–96.
- Kotański, Z., 1956. High-Tatric Campilian in the Tatra Mts. (In Polish, English summary). *Acta Geologica Polonica*, 6: 65–73.
- Kotański, Z., 1959a. Stratigraphical sections of the High-Tatric series in the Polish Tatra Mountains. (In Polish, English summary). *Biuletyn Instytutu Geologicznego*, 139: 1–160.
- Kotański, Z., 1959b. Contributions to the tectonics of the High-

- Tatric series. (In Polish, English summary). *Biuletyn Instytutu Geologicznego*, 149: 159–181.
- Kotański, Z., 1961. Tektogeneza i rekonstrukcja paleogeografii pasma wierzchowego w Tatrach. (In Polish, French summary). *Acta Geologica Polonica*, 11: 187–476.
- Kral, J., 1977. Fission track ages of apatites from some granitoid rocks in West Carpathians. *Geologický Sborník*, 28: 269–276.
- Książkiewicz, M., 1968. Observations on jointing in the Flysch Carpathians. (In Polish, English summary). *Rocznik Polskiego Towarzystwa Geologicznego*, 38: 335–384.
- Książkiewicz, M., 1972. *Budowa geologiczna Polski. T. IV. Tektonika, cz. 3. Karpaty*. (In Polish). Wydawnictwa Geologiczne, Warszawa, 228 pp.
- Lefeld, J., 1979. Trias serii wierzchovej. (In Polish). In: *Przewodnik LI Zjazdu PTG, Zakopane 13-15 września 1979*. Wydawnictwa Geologiczne, Warszawa: 27–31.
- Lefeld, J., 1997. Tektogeneza Tatr. Cykl alpejski. (In Polish). In: *Przewodnik LXVIII Zjazdu PTG, Zakopane, 2-4 października 1997*. Pol. Tow. Geol., Warszawa: 16–22.
- Lefeld, J., Gaździcki, A., Iwanow, A., Krajewski, K. & Wójcik, K., 1985. High-Tatric Succession. In: Jurassic and Cretaceous lithostratigraphic units of the Tatra Mountains. *Studia Geologica Polonica*, 84: 10–37.
- Mastella, L., 1988. Structure and evolution of Mszana Dolna tectonic window, Outer Carpathians, Poland. (In Polish, English summary). *Annales Societatis Geologorum Poloniae*, 58: 53–173.
- Mastella, L. & Konon, A., 2002. Jointing in the Silesian nappe (Outer Carpathians, Poland) – paleostress reconstruction. *Geologica Carpathica*, 53: 315–325.
- Mastella, L. & Zuchiewicz, W., 2000. Jointing in the Dukla Nappe (Outer Carpathians, Poland): an attempt at palaeostress reconstruction. *Geological Quarterly*, 44: 377–390.
- Mastella, L., Zuchiewicz, W., Tokarski, A. K., Rubinkiewicz, J., Leonowicz, P. & Szczesny, R., 1997. Application of joint analysis for paleostress reconstructions in structurally complicated settings: Case study from Silesian nappe, Outer Carpathians (Poland). *Przegląd Geologiczny*, 45: 1064–1066.
- Murray, F. N., 1967. Jointing in sedimentary rocks along The Grand Hogback monocline, Colorado. *Journal of Geology*, 75: 340–350.
- Ortner, H. & Reiter, F. & Acs, P., 2002. Easy handling of tectonic data: the programs Tectonics VB for Mac and Tectonics FP for Windows™. *Computers & Geosciences*, 28: 1193–1200.
- Piotrowski, J., 1978. Mesostructural analysis of the main tectonic units of the Tatra Mountains along the Kościeliska valley. (In Polish, English summary). *Studia Geologica Polonica*, 55: 1–90.
- Price, N. J., 1959. Mechanics of jointing in rocks. *Geological Magazine*, 96: 149–167.
- Price, N. J., 1966. *Fault and joint development in brittle and semi-brittle rock*. Pergamon Press, 176 pp.
- Price, N. J. & Cosgrove, J. W., 1990. *Analysis of geological structures*. Cambridge University Press, Cambridge, 502 pp.
- Rabowski, F., 1959. High-Tatric series in Western Tatra. (In Polish, English summary). *Prace Instytutu Geologicznego*, 27: 1–178.
- Reiter, F. & Acs, P., 2000. *Tectonics FP, ver. 1.6. Structural analysis software*.
- Riedel, W., 1929. Zur Mechanik geologischer Brucherscheinungen. *Zentralbl. Min. Geol. Pal., Abt. B.*, 509 pp.
- Roniewicz, P., 1959. Sedimentary characteristics of the High-Tatric Seis. (In Polish, English summary). *Acta Geologica Polonica*, 9: 301–317.
- Roniewicz, P., 1963. Flora remnants and fragments of granite in the High-Tatric Seis in the Tatra Mountains. (In Polish, English summary). *Biuletyn Geologiczny Uniwersytetu Warszawskiego*, 3: 274–284.
- Roniewicz, P., 1966. Lower Werfenian (Seisian) clastics in the Tatra mountains. (In Polish, English summary). *Acta Geologica Polonica*, 16: 1–90.
- Roniewicz, P., 1997. Trias dolny (werfen). (In Polish). In: *Przewodnik LXVIII Zjazdu PTG, Zakopane, 2-4 października 1997*. Pol. Tow. Geol., Warszawa: 44–46.
- Rubinkiewicz, J. 1998. Development of joints in Silesian nappe (Western Bieszczady, Carpathians, SE Poland). (In Polish, English summary). *Przegląd Geologiczny*, 46: 820–826.
- Sperner, B., Ratschbacher, L. & Nemčok, M., 2002. Interplay between subduction retreat and lateral extrusion: Tectonics of the Western Carpathians. *Tectonics*, 21 (6), 1051, doi: 10.1029/2001TC901028.
- Śmigieński, M., 2003. Reconstruction of geological structural parameters from large data sets. (In Polish, English summary). *Przegląd Geologiczny*, 51: 673–677.
- Turnau-Morawska, M., 1955. Remarks concerning sedimentation of the Werfen Beds in Tatra. (In Polish, English summary). *Rocznik Polskiego Towarzystwa Geologicznego*, 23: 37–52.
- Twiss, R. J. & Moores, E. M., 1992. *Structural Geology*. W. H. Freeman and Comp., New York, 532 pp.
- Uchman, A., 2004. Tetry, ich skały osadowe i badania sedymentologiczne. (In Polish). In: *Geologia Tatr: Ponadregionalny kontekst sedymentologiczny. Polska Konferencja Sedymentologiczna. VIII Krajowe Spotkanie Sedymentologów, Zakopane, 21-24 czerwca 2004*. Pol. Tow. Geol., ING UJ, Kraków: 5–21.
- Vaškovský, I., 1977. *Kvartér Slovenska*. (In Slovak). Geologický Ústav Dionýza Štúra, Bratislava, 249 pp.
- Zuchiewicz, W., 1997a. Reorientation of the stress field in the Polish Outer Carpathians in the light of joint pattern analysis. (In Polish, English summary). *Przegląd Geologiczny*, 45: 105–109.
- Zuchiewicz, W., 1997b. Distribution of jointing within Magura Nappe, West Carpathians, Poland, in the light of statistical analysis. (In Polish, English summary). *Przegląd Geologiczny*, 45: 634–638.
- Zuchiewicz, W., 1998. Cenozoic stress field and jointing in the Outer West Carpathians, Poland. *Journal of Geodynamics*, 26: 57–68.
- Zuchiewicz, W. & Henkiel, A., 1993. Orientation of late Cenozoic stress field axes in the light of joint pattern analysis in SE part of the Polish Carpathians. (In Polish, English summary). *Annales Universitatis Mariae Curie-Skłodowska, Sectio B*, 48: 311–348.

## Streszczenie

### EWOLUCJA SPĘKAŃ I USKOKÓW W OBREBIE WERFENSKICH PIASKOWCÓW KWARCYTICZNYCH – PRZYKŁAD Z POKRYWY AUTOCHTONICZNEJ TATR POLSKICH

Jacek Rubinkiewicz & Mirosław Ludwiniak

W niniejszym artykule przeprowadzono analizę spękań i uskoku w słabo zaburzonych tektonicznie piaskowcach kwarcyticznych werfenu. Piaskowce te rozpoczynają profil jednostki autochtonicznej (Tatricum) w Tatrach polskich, która leży bezpośrednio na trzonie krystalicznym.

W wyniku przeprowadzonych badań, polegających na analizie geometrycznej i genetycznej spękań i uskoków odtworzono pola paleonaprężeń i etapy ewolucji tych struktur w powiązaniu z ogólnie przyjętymi etapami ewolucji Tatr.

Najstarszymi spękaniami są spękania ścięciowe systemu S, które powstały w wyniku kompresji o kierunku SSW–NNE w skałach leżących niemal poziomo lub lekko wychylonych ku północy. W etapie tym mogły powstawać również uskoki zespołu F<sub>1</sub> w wyniku poślizgów wzdłuż powierzchni uławicenia lub bliskich tym powierzchniom. Miało to miejsce po wczesnym turonie, a przed koniakiem. W końcowej fazie tego etapu lub po nim mogło dojść do powstania głównych stref uskoków przesuwczych, łącznie ze strefą dyslokacyjną Ornaku.

Kolejny etap ewolucji omawianych struktur związany był z rotacyjnym wypiętrzeniem Tatr, trwającym od późnego miocenu. Sukcesywnie zaczęły powstawać spękania zespołu L w stopniowo wypiętrzających się skałach werfenu, w wyniku działania ekstensji o średnim kierunku SSW–NNE. W tym czasie doszło również do powstania uskoków normalnych systemu F<sub>2</sub>, z równoczesnym otwieraniem się części ze spękań systemu S oraz odmłodzeniem uskoków zespołu F<sub>1</sub>.

W ostatnim etapie ewolucji (plejstocen? – dziś) powstawały osuwiska konsekwentno-strukturalne, powodujące skręcenia pakietów warstw łącznie z występującymi tu spękaniami. Mogło również dojść do reaktywacji niektórych uskoków zespołu F<sub>1</sub>.